Available online at www.sciencedirect.com
SCIENCE DIRECT
International Journal of Mass Spectrometry 253 (2006) 79–86
International Journal of Mass Spectrometry
www.elsevier.com/locate/ijms

Electron impact ionization mass spectrometry of aliphatic alcohol clusters in helium nanodroplets

Shengfu Yang, Scott M. Brereton, Andrew M. Ellis *

Department of Chemistry, University of Leicester, University Road, Leicester LE1 7RH, UK

Received 13 December 2005; received in revised form 20 February 2006; accepted 20 February 2006
Available online 29 March 2006

Abstract

Electron impact ionization mass spectrometry has been applied for the first time to a range of molecular clusters inside helium nanodroplets. The clusters chosen for investigation are clusters of aliphatic alcohols. Fragmentation channels for the cluster cations in helium droplets differ significantly from previous findings in the gas phase. In addition to formation of abundant $(ROH)_nH^+$ ions, as already reported in gas phase studies, there are also important contributions from $(ROH)_n^+$ and $(ROH)_{n-1}RO^+$. The observation of substantial quantities of parent cluster ions, $(ROH)_n^+$, has not been reported previously and shows that helium nanodroplets, in combination with electron impact ionization, form a potentially useful source of metastable ions in the gas phase. The survival of these intact alcohol cluster ions is attributed to rapid evaporative cooling of the ions by the helium before they can react to produce $(ROH)_{n-1}H^+ + RO$. The major enhancement of the $(ROH)_{n-1}RO^+$ fragment channel when compared with gas phase cluster studies is attributed to a cage effect by the surrounding helium atoms. This favours the loss of a hydrogen atom by α-cleavage over the loss of a larger hydrocarbon fragment, although both channels are observed.

Keywords: Helium nanodroplet; Electron impact ionization; Molecular cluster; Ion fragmentation

1. Introduction

Liquid helium nanodroplets have demonstrated a number of unique properties. They possess an ultra-low temperature of 0.37 K for ^{4}He, which is well below the λ temperature of liquid helium ($T_\lambda = 2.17$ K under the saturated vapour pressure [1]). The resulting superfluidity allows molecules trapped within the droplets to translate, vibrate and rotate, as they would in the gas phase [2–7]. In addition, helium droplets are also able to rapidly release excess energy through evaporation of helium atoms. Consequently, warm molecules entering helium droplets can be quickly cooled down to the ambient temperature of the liquid helium if the droplet is sufficiently large.

Recently, there has been considerable interest in the electron impact ionization of molecules trapped inside large helium droplets in molecular beams. The ionization process is thought to begin with an electron striking a helium atom on the surface or inside the droplet [8–10]. The resulting positive charge undergoes a random walk and can hop from atom to atom several times before becoming localized, forming either a helium cluster cation or transferring the charge to an adjacent embedded molecule. Since the first ionization energy of a helium atom is generally far larger than that of a molecule, charge transfer leads to the release of several eV of excess energy. Ion fragmentation may result but excess energy may also be dissipated by evaporative loss of helium atoms, which can cool the parent ion and lessen the degree of fragmentation. The effectiveness of the helium in 'softening' the ionization process is dependent on the relative rates of evaporative cooling versus ion fragmentation.

Janda and co-workers carried out the first systematic studies of the electron impact (EI) ionization mass spectra of both pure and doped helium droplets [10–12]. This work focused mainly on the heavier noble gas atoms and their clusters in helium droplets, but also included was a report of soft ionization of NO dimers, the parent ion of which is almost entirely fragmented in the gas phase but which remains largely intact when ionized in helium droplets composed of ≥15,000 helium atoms [10].

More recently, Miller and co-workers have begun to explore the mechanism of ion cooling in helium nanodroplets following EI ionization. In a detailed investigation of the EI ionization

* Corresponding author. Tel.: +44 116 2522138; fax: +44 116 2523789.
E-mail address: andrew.ellis@le.ac.uk (A.M. Ellis).

1387-3806/$ – see front matter © 2006 Elsevier B.V. All rights reserved.
doi:10.1016/j.ijms.2006.02.019

of helium droplets doped with triphenylmethanol, a substantial change in the fragmentation pattern was observed compared with EI ionization of the isolated molecule [13]. These measurements were carried out for a variety of droplet sizes and it was found that the softening effect increased as the size of the droplet increased. However, the cooling ability did not increase in proportion to the number of helium atoms, but instead becomes less effective per atom as the droplet size increased. Very recently a study of the cooling of HCN ions in helium nanodroplets by the Miller group [14], using the technique of optically selected mass spectrometry [15], has revealed similar information. These data have been interpreted in terms of an explosive evaporation process once the charge is transferred onto the molecule. It appears that helium atoms leaving the droplet in this 'explosion' may possess energies well in excess of the energy (ca. 5 cm^{-1}) which binds each helium atom to the droplet. This cooling mechanism is most effective for small droplets, where helium atoms can escape relatively easily. Larger droplets will provide more of an obstacle to release of this energy and one outcome may be fission of the droplet into smaller fragments, thereby ultimately removing some of the cooling capacity of the original droplet.

To try and discover if soft or hard ionization is the norm for molecules encased in helium droplets, we have recently carried out electron impact ionization mass-spectrometry studies of two series of molecules in our laboratory. In one case the focus was on haloalkanes [16] and in the other small and medium-sized alcohols and ethers were investigated [17]. For haloalkanes, no major softening effect was found although the relative branching ratios of several fragmentation processes were altered. In particular, some fragmentation channels were significantly suppressed while others were enhanced. For example, in the case of 1,2-dichloroethane, the channel involving loss of a single chlorine atom from the parent ion is much more important in helium droplets when compared with the gas phase mass spectrum. In contrast, the HCl-loss channel, which is the major product channel in the gas phase, is severely depleted in helium droplets. For aliphatic alcohols and ethers, significant differences between helium droplets and the gas phase were observed. One of the notable findings was that channels involving loss of a single hydrogen atom become far more prominent in helium droplets compared with the gas phase. This was attributed to a dynamical effect in which the small scattering cross-section of hydrogen atoms compared with larger fragments increases the probability of the former being ejected. Furthermore, the parent ions are more abundant for most alcohols compared with the gas phase. This was found to be at its most dramatic for cyclopentanol and cyclohexanol, where the parent ions switched from being minor products in the gas phase spectra to being the major products in the helium droplet spectra. The difference in fragmentation patterns between the gas phase and helium droplets was attributed to a combination of evaporative cooling by helium droplets and a partial cage effect by the more tightly bound helium atoms in the solvent layer immediately surrounding the molecular ion.

In this study we extend our previous work on alcohol monomers to aliphatic alcohol clusters in helium droplets. This work constitutes the first detailed study of the electron impact ionization of a series of molecular clusters embedded in helium droplets. Previous gas-phase studies of the ionization of alcohol cluster ions can be divided into three groups: (1) early multiphoton ionization studies [18–20], (2) more recent VUV near-threshold single-photon ionization studies [21–23] and (3) electron impact investigations [24–27]. This prior work has focused mainly on methanol clusters, but some studies of clusters of the heavier alcohols have also been reported. The most extensive previous study, in terms of the range of alcohol molecules explored, was by Shukla and Stace [24]. This team investigated a series of primary, secondary and tertiary alcohol clusters, which were formed in a supersonic jet expansion and probed by EI mass spectrometry at an impact energy of 70 eV. In all previous studies of the ionization of alcohol clusters, including that of Shukla and Stace, the dominant products were found to be the protonated alcohol cluster ions, $(ROH)_nH^+$. The unprotonated parent ions, $(ROH)_n^+$, are very minor products even when near-threshold photoionization is employed [21–23]. When compared with photoionization, the much larger excess energies generated by standard 70 eV electron impact ionization tends to produce a greater degree of ion fragmentation. Various fragmentation channels have been observed, including H_2O elimination reactions and α-cleavage processes [24].

EI ionization of helium droplets doped with alcohol clusters reveals some similarities with previous gas phase studies along with some important differences. Protonated parent cluster ions remain the major products but new processes, such as the α-cleavage of H atoms, become important when the ions are encased in helium. Furthermore, the formation of unprotonated parent cluster ions is an important channel for all but one of the alcohols investigated. The results show that liquid helium nanodroplets are not able to fully quench fragmentation, but they do have a marked impact on branching ratios for several reaction channels.

2. Experimental details

A pulsed helium droplet source has been employed, which is similar in design to the pulsed source developed by Vilesov and co-workers [28]. Full details have been provided elsewhere [16,17,29] so only a concise account is given here. In a typical experiment a modified commercial pulsed valve, cooled by a closed-cycle cryostat, is maintained at a typical operating temperature of ∼11 K. High purity helium, at a stagnation pressure of 20 bar, is expanded through the pulsed nozzle to generate short (<200 μs) pulses of helium nanodroplets at a repetition rate of 10 Hz. For the chosen expansion conditions, the average droplet size has been estimated as ∼60,000 helium atoms [17].

The expanding helium droplets are skimmed to form a droplet beam and then enter a pickup cell, where analyte gases are added. The alcohols were bought from standard chemical suppliers with a minimum purity of 97%, and in most cases better than 99%. Each liquid sample was placed in a small cylindrical stainless steel container and degassed thoroughly prior to use. To minimize leakage of air into the sample vessel, helium carrier gas was added at a pressure in excess of 1 bar. This mixture of carrier gas plus headspace vapour is bled into the pickup cell using two needle valves in series to achieve fine control of the pressure. The

local pressure is monitored by an ion gauge located on a tube on the opposite side of the pickup cell from the gas inlet. Typical partial pressures of the alcohols in these experiments were in the region of 10^{-6} mbar, which is about one order of magnitude higher than in our previous work on alcohol monomers [17].

Mass spectra were recorded using a reflectron time-of-flight mass spectrometer with a total ion flight path of 2 m. This mass spectrometer was built by Kore Technology (Ely, UK) and is equipped with an electron impact source. The delay between the opening of the pulsed valve and the firing of the electron impact source was adjusted by a delay generator to ensure that the arrival of the gas pulse in the mass spectrometer source region was correctly synchronised with the firing of the electron beam. All measurements were made at an electron impact energy of 70 eV.

3. Results

Experiments have been carried out for clusters of the following aliphatic alcohols: methanol, ethanol, 1-propanol, 1-butanol, 1-pentanol, 2-methyl-1-propanol, 2-propanol, 2-butanol, 2-pentanol and tertiary butanol. These particular molecules were chosen partly to allow comparison with the earlier gas phase work, especially the electron impact study reported by Shukla and Stace [24]. For the large helium droplets employed in this work, the ion signals were very weak. Consequently, extensive averaging was used, each reported spectrum comprising an average of 10,000 individual scans.

Before discussing specific features of the helium droplet mass spectra, some of the common observations seen for the alcohol clusters are highlighted. As an illustration, Fig. 1 shows an EI mass spectrum obtained with 1-butanol in helium droplets. At low resolution, the dominant features are peaks that are clearly derived from a series of cluster ions. As the mass increases the cluster ions decrease in abundance until, in the region of the 1-butanol heptamer (not shown in Fig. 1), the signal becomes negligibly small. An expanded view of the region near the mass of the parent cluster ion reveals several peaks, the most intense of which is due to the protonated cluster ion, $(ROH)_nH^+$, but there are also sizeable contributions from $(ROH)_n^+$ and $(ROH)_{n-1}RO^+$. This 'triplet' structure is seen for all but one of the alcohols investigated in this work.

The high intensities of the $(ROH)H^+$ ions are in line with previous gas phase studies, which find the protonated parent cluster ions to be by far the most abundant species. However, the other two components of the 'triplet' are more intriguing. The formation of substantial proportions of parent cluster ions, $(ROH)_n^+$ for all values of n is a unique feature of ionization in helium droplets. In addition, the abundance of $(ROH)_{n-1}RO^+$ ions is unusual and was not observed in the earlier gas phase work. We have reported previously that alcohol monomers inside helium droplets have an increased tendency to lose a hydrogen atom on ionization when compared with the gas phase [17]. This finding was tentatively attributed to a partial cage effect by the helium droplets. This differential cage effect reflects the scattering cross-sections of the various departing products with the surrounding helium. Uncharged atomic fragments will find escape from the solvation cage much easier than molecular fragments because of the smaller helium scattering cross-sections for the former. This will be especially true for hydrogen atoms and this is the likely reason for the prominent appearance of $(ROH)_{n-1}RO^+$ ions in the helium nanodroplet mass spectra. In other words, these ions are formed by the α-cleavage reaction

$$(ROH)_n + He^+ \rightarrow (ROH)_{n-1}R'CH_2{=}O^+H + H + He. \quad (1)$$

In addition to $(ROH)_nH^+$, $(ROH)_n^+$ and $(ROH)_{n-1}RO^+$, other product ions can be seen in the mass spectrum in Fig. 1 and will be discussed later.

The findings for specific alcohols will now be described starting with the primary alcohols.

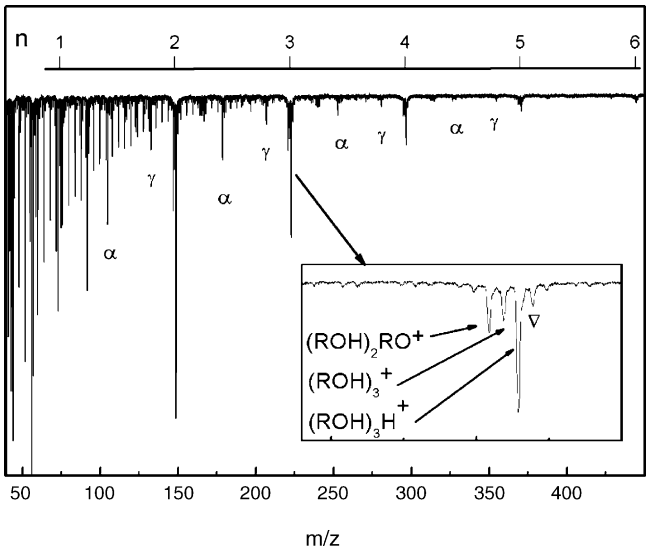

Fig. 1. Electron impact mass spectrum of 1-butanol clusters in helium droplets. In addition to helium cluster ion peaks, He_n^+, which form an extensive series of closely spaced peaks with significant intensities at $m/z < 250$, the main series of peaks are due to alcohol cluster ions and their fragments. The expanded region focuses on peaks in the vicinity of the 1-butanol parent trimer ion and shows the 'triplet' structure that is prominent for most of the alcohol clusters. The additional peak in the inset, labeled ∇, is the ^{13}C isotopomer of the protonated trimer ion. Peaks marked α are assigned to the α-cleavage products $(1\text{-BuOH})_nCH_2O^+H$, and those marked by γ correspond to C_γ—C_δ bond cleavage, forming $(1\text{-BuOH})_{n-1}C_3H_6O^+H$ ions.

4. Primary alcohols

4.1. Methanol

Fig. 2 shows part of the EI mass spectrum recorded for methanol clusters. As with the 1-butanol spectrum in Fig. 1, the spectrum for methanol clusters in helium nanodroplets shows a triplet structure near the parent cluster ion positions. The assignment of these features parallels 1-butanol, with $(MeOH)_nH^+$, $(MeOH)_n^+$ and $(MeOH)_{n-1}MeO^+$ being responsible. The EI mass spectrum of small methanol clusters in helium nanodroplets has been reported on previously as part of an infrared spectroscopy study by Behrens et al. of uncharged methanol clusters in liquid helium [30]. However, while the protonated ions $(MeOH)_nH^+$ were briefly discussed, and indeed were used

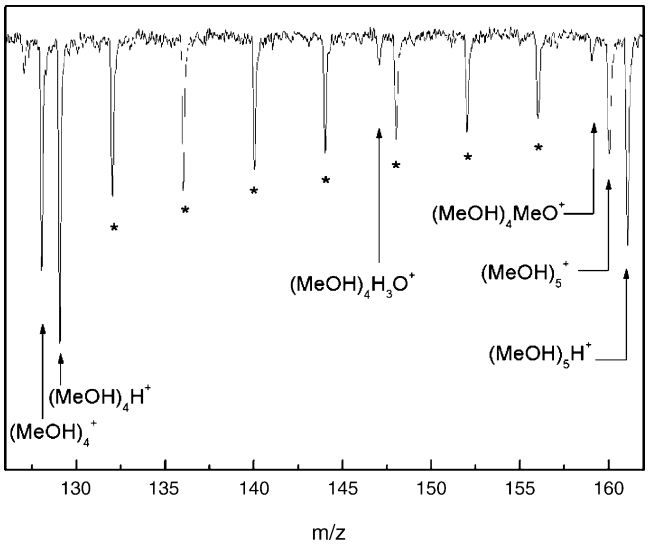

Fig. 2. A portion of the mass spectrum of methanol clusters in helium droplets. The peaks marked by asterisks (*) are helium cluster cations. Triplet structure in the parent ion region is clearly visible at both ends of the spectrum, with $(MeOH)_nH^+$ providing the strongest peak in each case. The only other significant organic ions are due to $(MeOH)_nH_3O^+$.

for the detection of IR transitions in the neutral clusters using depletion spectroscopy, no mention was made of accompanying strong signals of parent cluster ions, $(MeOH)_n^+$. The main difference between the study by Behrens et al. and the present work is the use of much larger helium droplets in the latter (60,000 versus 2700), which may be more conducive to the formation of parent ion clusters.

The relative abundances of these types of ions are noticeably different for methanol when compared with 1-butanol. The α-cleavage product $(MeOH)_{n-1}MeO^+$ has a much lower abundance than $(MeOH)_n^+$, whereas for 1-butanol the α-cleavage product was found to be more abundant than the unprotonated parent cluster ions. The relative intensities of the triplet peaks remain the same for all cluster sizes up to the maximum observed, $n = 13$.

Away from the parent cluster ion region, the only detectable product is a weak feature appearing 19 mass units above each parent cluster ion. This is attributed to $(MeOH)_nH_3O^+$, which has been reported in previous work [25] and which could be formed by the process

$$(MeOH)_{n+m+2}H^+ \rightarrow (MeOH)_nH_3O^+ + Me_2O + (MeOH)_m. \quad (2)$$

However, we add that substantial amounts of water vapour were also detectable in the mass spectrum despite efforts to minimize this contaminant. It is therefore possible that some of the $(MeOH)_nH_3O^+$ ions result from the ionization of $(MeOH)_iH_2O$ heteroclusters formed in the helium droplets, where $i > n$. Electron impact ionization of the helium droplet could yield $(MeOH)_nH_3O^+$ by the process

$$(MeOH)_iH_2O + He^+ \rightarrow (MeOH)_nH_3O^+ + (MeOH)_{i-n} + MeO + He. \quad (3)$$

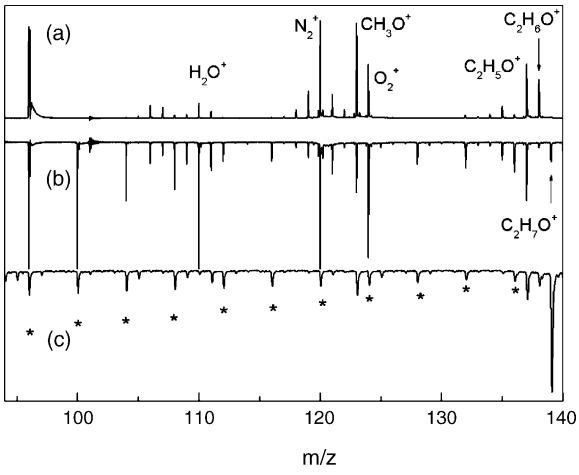

Fig. 3. Mass spectra of ethanol for (a) ethanol in the gas phase and (b) the monomer in helium droplets. Spectrum (c) is for ethanol clusters in helium droplets. Peaks marked by asterisks (*) in (c) are due to helium cluster cations. To facilitate comparison of the spectra, the mass axes for (a) and (b) have been shifted by $m/z = +92$ such that the ethanol monomer cation peak is aligned with the position of the ethanol trimer cation in spectrum (c).

Small quantities of hydrated cluster ions of the type formed in reaction (3) were also observed for most of the other alcohols studied in the present work.

4.2. Ethanol

A comparison of EI fragmentation patterns for ethanol monomer in the gas phase, ethanol monomer in helium droplets, and ethanol clusters in helium droplets, is provided in Fig. 3. Again a triplet structure is observed in the parent cluster ion region, with a ratio of $(EtOH)_nH^+$, $(EtOH)_n^+$ and $(EtOH)_{n-1}EtO^+$ ions that more closely matches the corresponding ion ratios for 1-butanol than did methanol.

A variety of weak fragment peaks can be identified in the helium droplet mass spectrum. However, the principal fragment peak is 15 Da below each parent ion peak (at 123 Da in Fig. 3c). This fragment ion is the cluster analogue of the most abundant ion seen in the helium droplet mass spectrum of ethanol monomer and by analogy can be assigned to the α-cleavage product formed in the reaction

$$(C_2H_5OH)_n^+ \rightarrow (C_2H_5OH)_{n-1}CH_2O^+H + CH_3. \quad (4)$$

4.3. 1-Propanol

The EI mass spectrum of 1-propanol clusters in helium droplets is similar to that of ethanol. Besides the triplet structure in the parent cluster ion region, the main fragment peak corresponds to the oxonium ion $(C_3H_7OH)_nCH_2O^+H$, which is formed by α-cleavage.

4.4. 2-Methyl-1-propanol

For 2-methyl-1-propanol clusters the helium droplet mass spectrum is dominated by the protonated cluster ions $(ROH)_nH^+$. By comparison, $(ROH)_{n-1}RO^+$ and $(ROH)_n^+$ signals are much

weaker, with the latter being the weakest of the 'triplet' peaks at roughly an order of magnitude smaller than the adjacent $(ROH)_nH^+$ peak. Several fragments are observed at even lower relative intensities, the principal one being the oxonium ion $(ROH)_{n-1}CH_2O^+H$. Small but significant peaks are also observed which can be attributed to $(ROH)_{n-1}CH_3^+$ ions These are surprising products requiring C_β–C_γ bond fission, an event some distance from the region of intermolecular hydrogen bonding. It is conceivable that a cage effect in helium nanodroplets aids the formation of these ions by allowing the CH_3 fragment to recombine with the alcohol cluster ion after C_β–C_γ bond fission.

4.5. 1-Butanol

In addition to the triplet structure discussed earlier, the 1-butanol spectrum in Fig. 1 shows only two additional series of fragment peaks. This is a much simpler fragmentation pattern than found for the monomer in helium droplets [13,17], where there are many fragments with substantial abundances, including some whose analogues in the cluster spectrum are barely detectable. The peaks marked with the label α are the α-cleavage products $(BuOH)_{n-1}CH_2O^+H$ while the series marked by γ seems to correspond to the products $(BuOH)_{n-1}(CH_2CH_2CH_2OH)^+$, which would be formed by fission of the C_γ–C_δ bond in one of the butanol units. In the monomer mass spectrum the corresponding fragmentation product is observed but is not prominent. Consequently, there seems to be a degree of fragmentation selectivity in the cluster mass spectrum that is missing for the monomer. Since formation of $(BuOH)_{n-1}(CH_2CH_2CH_2OH)^+$ was not reported in the gas phase study of alcohol clusters by Shukla and Stace [24], we conclude that the helium matrix is responsible for the fragmentation selectivity.

5. Secondary alcohols

A typical mass spectrum of secondary alcohols is shown in Fig. 4, with 2-propanol as the example. The series a_n consists of the triplet structure in the parent cluster ion region analogous to that already reported for the primary alcohols. The peaks labeled b_n are due to loss of CH_3 from $(2\text{-PrOH})_n$ by α-cleavage to give $(2\text{-PrOH})_{n-1}(CH_3CHOH)^+$. Shukla and Stace have previously reported this α-cleavage process in the gas phase, but observed no α-cleavage beyond $n=6$ [24]. We see no such termination at $n=6$ and find that α-cleavage persists up to the largest 2-propanol clusters observed, which correspond to $n=8$.

The weak series c_n is more difficult to assign. One possibility is that these peaks result from ejection of an H_2O molecule from the aforementioned α-cleavage product, i.e.,

$$(2\text{-PrOH})_{n-1}(CH_3CHOH)^+ \rightarrow (2\text{-PrOH})_{n-1}(C_2H_3)^+ + H_2O \quad (5)$$

Fragmentation of the oxonium ions formed by 2-propanol clusters has been reported previously by Shukla and Stace, although only for $n=2$ was reaction (5) observed: larger clusters ejected acetaldehyde [24].

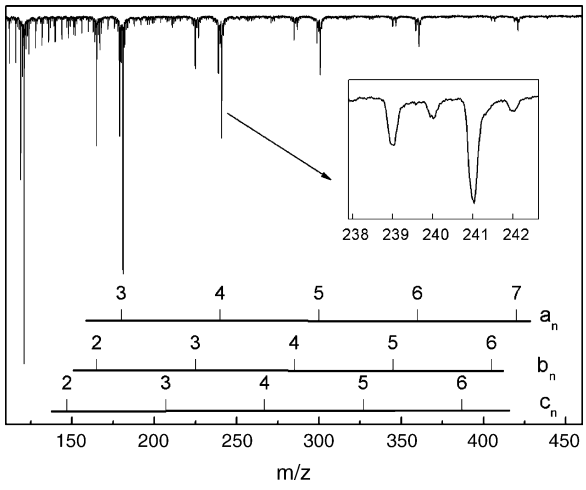

Fig. 4. Mass spectrum for 2-propanol clusters in helium droplets. The peaks designated a_n refer to the triplet features near each parent cluster ion position, with n being the number of monomer units. Series b_n is due to the α-cleavage of CH_3 from the parent cluster ions, $(2\text{-PrOH})_{n+1}$, and series c_n is assumed to result from further loss of H_2O from the α-cleavage products b_n.

Interestingly, each peak in the series b_n is accompanied by a weak partner 2 Da higher. This corresponds to the loss of CH from the unprotonated parent ion but it seems unlikely that this process occurs directly. An alternative is that CH_2 loss occurs from the protonated parent ion, but again this has no precedent in gas phase studies.

2-Butanol yields a cluster mass spectrum very similar to that of 2-propanol. However, in contrast to 2-propanol there are two hydrocarbon fragments that can be lost by α-cleavage, C_2H_5 or CH_3. Expulsion of the former gives the more abundant product, as would be expected by the usual predictive rules for α-cleavage based on the relative stabilities of the ejected radical fragments [31,32]. Moreover, a series of $(2\text{-BuOH})_nC_2H_5O^+\cdot H_2O$ peaks are also observed, similar to that of 1-butanol.

Like 2-butanol, clusters of 2-pentanol have three options for α-cleavage: expulsion of H, CH_3 or C_3H_7. Peaks due to all three possibilities give rise to the only three fragment ions observed in the mass spectra, with approximate relative branching ratios of 3:1:3, respectively, for these channels.

6. Tertiary alcohols

The only tertiary alcohol studied in this work was *t*-butanol; the mass spectrum obtained is shown in Fig. 5. Similar to the primary and secondary alcohols, α-cleavage is one of the dominant fragmentation channels in the cluster ion mass spectrum. However, there are also some important differences in the fragmentation pattern of *t*-butanol.

The most striking difference is the almost complete absence of the triplet structure around the position of the parent cluster ions. Instead the spectrum in this region is dominated by a single peak due to the protonated species $(t\text{-BuOH})_nH^+$. The absence of significant peaks due to H-loss from the parent cluster ions is simply because there is no α-hydrogen in *t*-butanol. This demonstrates categorically that the H-loss channels seen for the other alcohols arise from cleavage of the C_α–H bond.

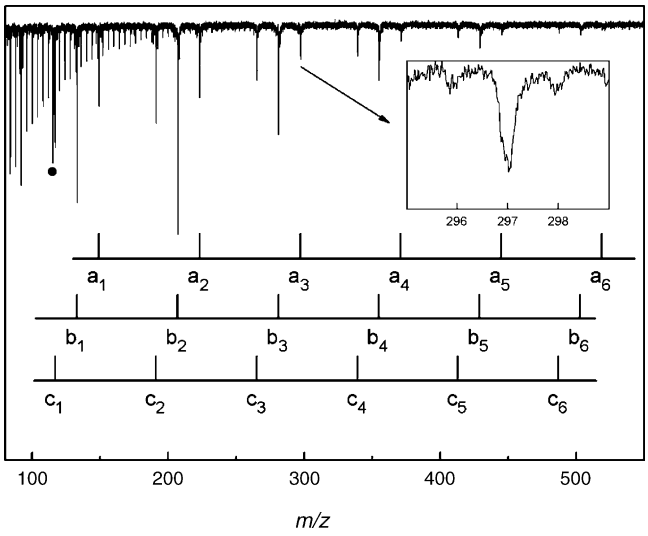

Fig. 5. Electron imapct mass spectrum of *t*-butanol clusters. The series a_n, b_n and c_n correspond to (*t*-BuOH)$_{n+1}H^+$, (*t*-BuOH)$_n(CH_3)_2COH^+$ and (*t*-BuOH)$_n(C_3H_7)^+$, respectively, with $n = 1$–6. There is an extra peak at $m/z = 115$ marked ● which is assigned to (*t*-BuOH)C_3H_5. Note that this peak only appears for $n = 1$.

In marked contrast to all the other alcohols studied the parent cluster ions, (*t*-BuOH)$_n^+$, make a very small contribution to the mass spectra.

Another interesting feature of the *t*-butanol cluster mass spectra is the large degree of fragmentation, with fragmentation products being more abundant than the protonated parent species, (*t*-BuOH)$_nH^+$. The mass spectrum of *t*-butanol monomer shows similar behaviour, with almost no detectable parent ion peak. As with the monomer, the most abundant ion corresponds to α-cleavage of one of the methyl groups to yield the product (*t*-BuOH)$_{n-1}(CH_3)_2COH^+$. Also significant are peaks corresponding to loss of OCH_3 to form (*t*-BuOH)$_{n-1}C_3H_7^+$. In both the gas phase spectrum of the monomer and the monomer spectrum in helium droplets the loss of OCH_3 has a smaller branching ratio than loss of C_3H_7. However, in the cluster spectrum derived from helium droplets this ordering is reversed and in fact no detectable loss of C_3H_7 is observed. This behaviour was not reported in the gas phase cluster study by Shukla and Stace [24], suggesting that the helium once again has a marked effect on the cluster ion fragmentation branching ratios.

Finally, we note that a relatively strong peak is observed 2 Da below that of (*t*-BuOH)$C_3H_7^+$, and in fact it has a greater abundance than (*t*-BuOH)$C_3H_7^+$. This additional peak is presumably due to loss of two hydrogen atoms from the aforementioned ion, although it is not clear whether these are lost from the alcohol unit or the hydrocarbon unit. Unusually, this process is not observed for higher clusters.

7. Discussion

A comparison of monomer and cluster mass spectra in the gas phase and in helium droplets has revealed considerable similarities in fragmentation channels accompanied by some important differences. Some of the differences in fragmentation behaviour are common to both the alcohol monomers and their clusters in helium droplets, and therefore much of the discussion employed previously for the monomers [17] will be transferable to the clusters. Consequently, the discussion here will focus on perhaps the most intriguing difference between the gas phase and helium droplet spectra for the alcohol clusters, the observation of significant amounts of parent cluster ions, (ROH)$_n^+$, alongside the more abundant protonated analogues, (ROH)$_nH^+$.

Previous studies of the electron impact ionization of methanol clusters in the gas phase have revealed no detectable parent methanol cluster ions [25,26]. Equally, in their investigation of ion products from a broader range of clusters, Shukla and Stace also observed no parent cluster ions for any of the alcohols studied [24]. However, parent alcohol cluster ions have been observed previously in the gas phase using near-threshold photoionization. Very weak signals from methanol dimer cations were reported in a photoionization study by Tsai et al. [21], while in a photoionization study of ethanol and 1-propanol clusters the alcohol dimer cations were observed but no higher parent cluster ions were detectable [23]. The survival of a substantial proportion of parent alcohol cluster ions in the present work is therefore a finding quite different from previous studies. This is most marked in the case of methanol, where parent cluster ions (MeOH)$_n^+$ are only moderately less abundant than the proton transfer dissociation product (MeOH)$_nH^+$.

Perhaps most relevant to the present work is a study of the electron impact ionization of Ar$_n$(MeOH)$_n$ clusters by Vaidyanathan et al. [27]. The mixed argon-methanol clusters were produced by co-expansion of methanol and the inert carrier gas through a supersonic nozzle. A variety of species were observed but they included methanol parent cluster ions, both in isolation and in Ar$_n$(MeOH)$_n^+$ heteroclusters. However, even at electron impact energies as low as 17 eV the parent cluster ion signals were relatively weak compared with other ions produced, most notably the protonated species (MeOH)$_nH^+$. The absence of unprotonated cluster ions such as (MeOH)$_n^+$ is often attributed to poor Franck-Condon factors for ionization due to large changes in equilibrium structure between the neutral cluster and the ion. Vertical ionization results in ions being produced with considerable excess vibrational energies, which then allow rapid conversion to the protonated species. In the specific case of (MeOH)$_2$, ab initio calculations predict that vertical ionization results in a cation with a total energy above that for (MeOH)H$^+$ + OMe [26]. The calculations show that the transition state for the process

$$[(MeOH)_2{}^+]_{vertical} \rightarrow (MeOH)H^+ + OMe \quad (6)$$

lies well below the combined energies of both reactants and products, so the above reaction is barrierless and would be expected to proceed rapidly. Unless some of the excess vibrational energy in the initially formed cation, $[(MeOH)_2{}^+]_{vertical}$, is quenched rapidly, reaction (6) is inevitable. The parent cluster ions therefore form a minimum on the potential energy surface but unless specifically stabilised in this minimum the system will proceed onwards to form the more stable protonated species.

The survival of parent cluster ions in the study by Vaidyanathan et al. [27] can be attributed to an indirect ionization process involving the argon atoms. An electron striking an argon atom may induce either direct ionization or electronic excitation and both of these processes can lead to subsequent ionization of a methanol molecule in contact with the argon atom. An argon cation can exchange charge with the molecule, leading to methanol cation formation along with the release of excess energy (equal to the difference in ionization energies of argon and methanol). Alternatively, electronically excited metastable argon can ionize the methanol by an intracluster Penning ionization process. Vaidyanathan present evidence in favour of an intracluster Penning ionization process, but the key point is that whichever ionization mechanism operates, the surrounding argon provides a means of removing the excess energy by evaporative loss of argon atoms. This process accounts for the stabilisation of parent methanol cluster ions.

A similar process is likely to be in operation in helium droplets. Superfluid liquid helium is an excellent thermal conductor and with sufficiently large droplets a large amount of energy can potentially be rapidly dissipated by evaporative loss of helium atoms. For molecules inside helium droplets the principal ionization mechanism following electron impact is thought to be charge exchange when the molecule comes into contact with He^+, rather than Penning ionization [33]. Given that the first ionization energies of alcohol clusters are in the region of 10 eV [19–21], charge transfer will deposit ~14 eV into the newly formed alcohol cluster ion. The helium droplets employed in the present work, which have an average of 60,000 helium atoms, are large enough to dissipate this energy fully. Assuming the energy removed by each helium atom is comparable to its binding energy to the droplet (ca. 5 cm^{-1}), then loss of 22,000 helium atoms would be required to remove this excess energy. However, with such a large excess energy of 14 eV a dissociative proton transfer of the type shown in reaction (6) is expected to occur on a timescale comparable to the vibrational period of the intermolecular hydrogen bond, i.e., ca. 1 ps. Such a process is irreversible in the absence of a cage effect and given the enormous rate of cooling apparently required it therefore seems remarkable at first sight that any parent alcohol cluster ions are detected in the helium nanodroplet experiments.

However, not all the excess energy needs to be dissipated on a ps timescale in order for significant quantities of the parent ions to survive. Instead, only part of this energy would need to be lost on an ultrafast timescale such that the rate of the dissociative proton transfer slows considerably. The requirement for an initial rapid loss of energy would be provided by the explosive cooling mechanism proposed by Miller and co-workers [14]. Having lost several eV of energy by this route, cooling thereafter of the cluster ion could continue at a much slower rate, most likely on a nanosecond timescale by normal evaporative loss of helium atoms [34], leading to the survival of some parent alcohol cluster ions. This two-step mechanism may account for the observation of substantial quantities of $(ROH)_n^+$ ions in the EI mass spectra of alcohol clusters in helium nanodroplets.

The stabilisation of cluster ions of the heavier alcohols by the liquid helium is less effective than for methanol. The most extreme case is that of *t*-butanol, where no parent cluster ions were observed at all. A photoelectron–photoion coincidence (PEPICO) study has shown that the *t*-butanol cation is unstable with respect to methyl loss even at the ionization threshold for the neutral molecule [35]. At threshold the ionization process deposits the cation onto a repulsive potential energy surface with respect to the $(t\text{-BuOH})_{n-1}(CH_3)_2COH^+ + CH_3$ dissociation limit with no apparent barrier along the dissociation coordinate. Thus, quenching by liquid helium could do nothing to halt this fragmentation and this explains why no *t*-butanol parent cluster ions are seen.

In principle, the stabilisation of some alcohol cluster ions in helium nanodroplets could provide a means of allowing their spectroscopic study for the first time. For example, specific $(ROH)_n^+$ ions ejected from helium droplets into a reflectron time-of-flight mass spectrometer flight tube via electron impact ionization could be selected for onward transmission by a standard pulsed mass gate. Subsequent spectroscopic excitation at the turning point in the reflector array could then be used to induce the intracluster reaction $(ROH)_n^+ \rightarrow (ROH)_{n-1}H^+ + RO$, providing sufficient is deposited into the initial ion. Laser photofragment spectroscopy of this type, in which the fragment $(ROH)_{n-1}H^+$ is detected in the return stage of the reflectron, would be similar to the proven laser photofragment spectroscopic technique for studying ions pioneered by Duncan (see, for example, refs. [36,37]).

8. Conclusions

Electron impact ionization mass spectrometry has been applied for the first time to molecular clusters encased in helium nanodroplets. Alcohol clusters were chosen for investigation, since these have been subjected to several previous mass spectrometry studies in gas phase environments. Fragmentation channels for the ions in helium droplets differ significantly from observations in the gas phase. In addition to formation of abundant $(ROH)_nH^+$ ions, as already reported in gas phase studies, there are also sizeable contributions from $(ROH)_n^+$ and $(ROH)_{n-1}RO^+$. The relative abundances of these ions are largely independent of the cluster size. The observation of parent cluster ions, $(ROH)_n^+$, is attributed to rapid evaporative cooling of the ions within the helium droplets before they can react to produce $(ROH)_{n-1}H^+ + RO$. A two-step mechanism is proposed which begins with an initial explosive event, immediately after charge has been transferred from a neighbouring He^+ ion, which rapidly removes several eV of energy from the initially formed ion. This is then followed by a slower evaporative cooling process. The formation of substantial quantities of $(ROH)_n^+$ cations suggests that helium nanodroplets, in combination with electron impact ionization, could be a useful source of metastable ions in the gas phase, e.g., for optical spectroscopy or experiments on ion-molecule reactions. The major enhancement of the $(ROH)_{n-1}RO^+$ fragmentation channel when compared with gas phase cluster studies is attributed to a cage effect by the surrounding helium atoms. The loss of a hydrogen atom by α-cleavage is favoured by the cage effect over the loss of a larger hydrocarbon fragment, although both channels are observed.

Acknowledgements

The authors are grateful to the UK Engineering and Physical Sciences Research Council for financial support of this work.

References

[1] J. Wilks, An Introduction to Liquid Helium, Clarendon Press, Oxford, 1970.
[2] J.P. Toennies, A.F. Vilesov, Ann. Rev. Phys. Chem. 49 (1998) 1.
[3] J.P. Toennies, A.F. Vilesov, Angew. Chem. Int. Ed. 43 (2004) 2622.
[4] R. Fröchtenicht, J.P. Toennies, A.F. Vilesov, Chem. Phys. Lett. 229 (1994) 1.
[5] A. Conjusteau, C. Callegari, I. Reinhard, K.K. Lehmann, G. Scoles, J. Chem. Phys. 113 (2000) 4840.
[6] S. Goyal, D.L. Schutt, G. Scoles, J. Phys. Chem. 97 (1993) 2236.
[7] R.E. Miller, Faraday Discuss. 118 (2001) 1.
[8] H. Buchenau, J.P. Toennies, J.A. Northby, J. Chem. Phys. 95 (1991) 8134.
[9] J. Seong, K.C. Janda, N. Halberstadt, F. Spiegelmann, J. Chem. Phys. 109 (1998) 10873.
[10] B.E. Callicoatt, D.D. Mar, V.A. Apkarian, K.C. Janda, J. Chem. Phys. 105 (1996) 7872.
[11] B.E. Callicoatt, K. Förde, L.F. Jung, T. Ruchti, K.C. Janda, J. Chem. Phys. 109 (1998) 10195.
[12] T. Ruchti, K. Förde, B.E. Callicoatt, H. Ludwigs, K.C. Janda, J. Chem. Phys. 109 (1998) 10679.
[13] W.K. Lewis, B.E. Applegate, J. Sztáray, B. Sztáray, T. Baer, R.J. Bemish, R.E. Miller, J. Am. Chem. Soc. 126 (2004) 11283.
[14] W.K. Lewis, R.J. Bemish, R.E. Miller, J. Chem. Phys. 123 (2005) 141103.
[15] W.K. Lewis, C.M. Lindsay, R.J. Bemish, R.E. Miller, J. Am. Chem. Soc. 127 (2005) 7235.
[16] S. Yang, S.M. Brereton, M.D. Wheeler, A.M. Ellis, J. Phys. Chem. A 110 (2006) 1791.
[17] S. Yang, S.M. Brereton, M.D. Wheeler, A.M. Ellis, Phys. Chem. Chem. Phys. 7 (2005) 4082.
[18] S. Morgan, A.W. Castleman, J. Am. Chem. Soc. 109 (1987) 2867.
[19] S. Morgan, R.G. Keesee, W. Castleman, J. Am. Chem. Soc. 111 (1989) 3841.
[20] P. Xia, M. Hall, T.R. Furiani, J.F. Garvey, J. Phys. Chem. 100 (1996) 12235.
[21] S.-T. Tsai, J.-C. Jiang, Y.T. Lee, A.H. Kung, S.H. Lin, C.-K. Ni, J. Chem. Phys. 111 (1999) 3434.
[22] Y.J. Shi, A.K. Das, B. Mallik, D. Lacey, R.H. Lipson, J. Chem. Phys. 116 (2002) 6990.
[23] S.-T. Tsai, J.-C. Jiang, M.-F. Lin, Y.T. Lee, C.-K. Ni, J. Chem. Phys. 120 (2004) 8979.
[24] A.K. Shukla, A.J. Stace, J. Phys. Chem. 92 (1988) 2579.
[25] M.S. El-Shall, C. Marks, L.W. Sieck, M. Meot-Ner, J. Phys. Chem. 96 (1992) 2045.
[26] S.Y. Lee, D.N. Shin, S.G. Gyeong, K.-H. Jung, K.W. Jung, J. Mass Spectrom. 30 (1995) 969.
[27] G. Vaidyanathan, M.T. Coolbaugh, W.R. Pfeifer, J.F. Garvey, J. Chem. Phys. 94 (1991) 1850.
[28] M.N. Slipchenko, S. Kuma, T. Momose, A.F. Vilesov, Rev. Sci. Instrum. 73 (2002) 3600.
[29] S. Yang, S.M. Brereton, A.M. Ellis, Rev. Sci. Instrum. 76 (2005) 104102.
[30] M. Behrens, R. Fröchtenicht, M. Hartmann, J.-G. Siebers, U. Buck, F.C. Hagemeister, J. Chem. Phys. 111 (1999) 2436.
[31] H. Budzikiewicz, C. Djerassi, D.H. Williams, Mass Spectrometry of Organic Compounds, Holden-Day Inc., San Francisco, 1967.
[32] F.W. McLafferty, F. Tureček, Interpretation of Mass Spectra, University Science Books, Mill Valley, CA, 1993.
[33] B.E. Callicoatt, K. Förde, T. Ruchti, L.F. Jung, K.C. Janda, N. Halberstadt, J. Chem. Phys. 108 (1998) 9371.
[34] D.M. Brink, S. Stringari, Z. Phys. D 15 (1990) 257.
[35] J.D. Shao, T. Baer, D.K. Lewis, J. Phys. Chem. 92 (1988) 5123.
[36] M.A. Duncan, Int. J. Mass Spectrom. 200 (2000) 545.
[37] M.A. Duncan, Int. Rev. Phys. Chem. 22 (2003) 407.